A low resolution model of fragment 1 from bovine prothrombin

Gustaf Olsson, Leif Andersen, Oliver Lindqvist, Lennart Sjölin, Staffan Magnusson*, Torben Ellebæk Petersen* and Lars Sottrup-Jensen*

Department of Inorganic Chemistry, Chalmers University of Technology, S-412 96 Göteborg, Sweden and **Department of Molecular Biology, University of Aarhus, DK-8000 Århus C, Denmark*

Received 8 July 1982

Fragment 1 *Prothrombin* *Structure* *Crystal* *Blood coagulation* *Thrombin*

1. INTRODUCTION

The primary structure of bovine prothrombin is completely known today. In normal prothrombin the first ten glutamic acids are modified into γ-carboxy glutamic acids [1]. By the activation of the zymogen prothrombin into the enzyme thrombin, Ca^{2+} and phospholipid are required [2]. The binding sites are located in the so-called fragment 1 part (residues 1–156), which contains all the modified glutamic acids [3] (fig.1). Fragment 1 is a well-defined fragment of prothrombin and shows essentially the same binding properties towards Ca^{2+} and phospholipid as prothrombin itself [4]. This indicates that the three-dimensional structure is conserved in fragment 1 also when released from prothrombin. Thus knowledge of the three-dimensional structure of fragment 1 would contribute to the understanding of the prothrombin activation. The present paper describes the X-ray structure determination of fragment 1 to a 4 A.U. resolution.

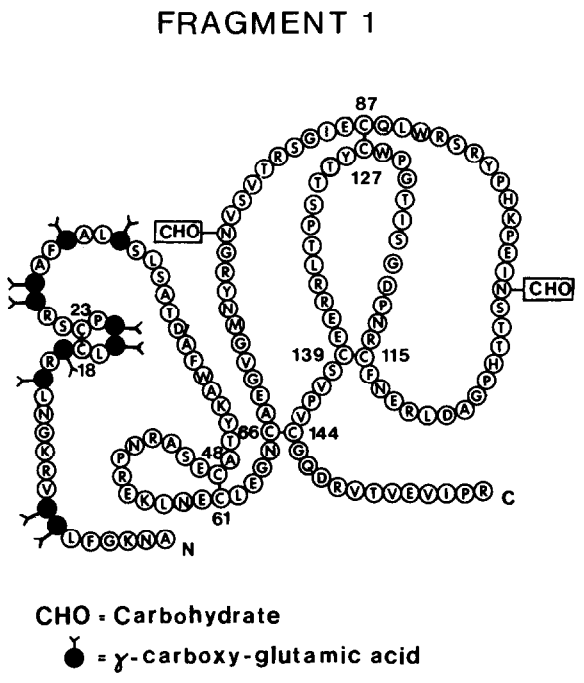

Fig.1. Amino acid sequence of fragment 1 from bovine prothrombin residue 1–156. The five disulfide bridges are indicated. The two carbohydrate sites are of equal size, about 20% of the molecular weight. Each ring denotes one amino acid residue.

2. EXPERIMENTAL

2.1. *Crystallization*

Fragment 1 was prepared from pure prothrombin by incubating purified thrombin (ratio 200:1, w/w) for two hours at 25°C [1]. The separation of fragment 1 from prothrombin 1 was performed with a DEAE-Sephadex A50 column eluated with a linear gradient of sodium chloride, resalted to 50 mM ammonium hydrogen carbonate on a Sephadex G-100 column at pH 8.3 and finally lyophilized and stored.

Large, stable crystals (fig.2) were grown in the pH range of 6.0–7.0 and in the presence of 100 mM Ca^{2+} using 100 mM sodium cacodylate as buffer and 8% (w/v) polyethylene glycol (PEG 6000) as precipitant. The crystallization technique

Published by Elsevier Biomedical Press
00145793/82/0000–0000/$2.75

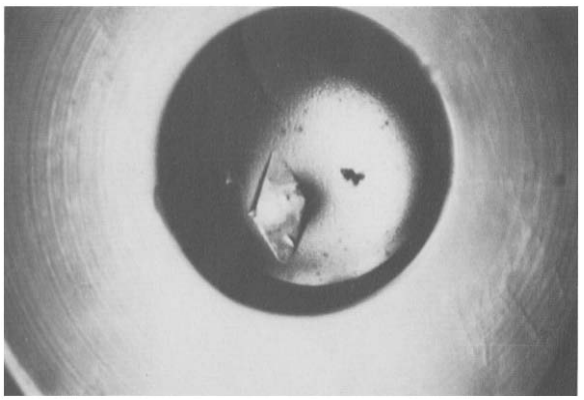

Fig.2. Bovine fragment 1 crystal. Length along the *c*-axis about 1.1 mm.

was vapor diffusion in so-called Lagerkvist cells [5].

At the early stages of the crystallization studies it was difficult to define reproducible conditions for crystal growth. Eventually, it was found that dissolving a few crystals in the freshly made protein solution, ensured reproducible results. This peculiarity motivated a reinvestigation of the amino acid composition using substance from dissolved crystals only. This showed that five amino acids were missing at the C-terminus and possibly some of the carbohydrate.

Another crystalline form of fragment 1 has been reported [6,7]. These crystals are tetragonal and have been obtained in the absence of calcium ions by dialysing the protein either against ammonium sulphate or a mixture of potassium and sodium hydrogen phosphate in neutral or slightly alkaline solutions.

2.2. *Data collection and processing*

The diffraction quality and the unit cell dimensions were investigated with a precession camera (cf. fig.3). Crystallographic data are summarized in table 1.

Three-dimensional diffraction data to a 2.8 A.U. resolution were collected at room temperature using the rotation method [8]. The crystals were rotated around the crystallographic *c*-axis and were exposed to graphite monochromated CuK_α radiation from a rotating anode. The X-ray was collimated by a 20 cm long collimator, 0.3 mm in diameter. A rotation angle of 3° was used for each film set and films were collected over a total rotation of 90°. Because of radiation damage a complete data set required two to three crystals. The approximately 400 reflections hidden in the blind region at this crystal setting were not collected.

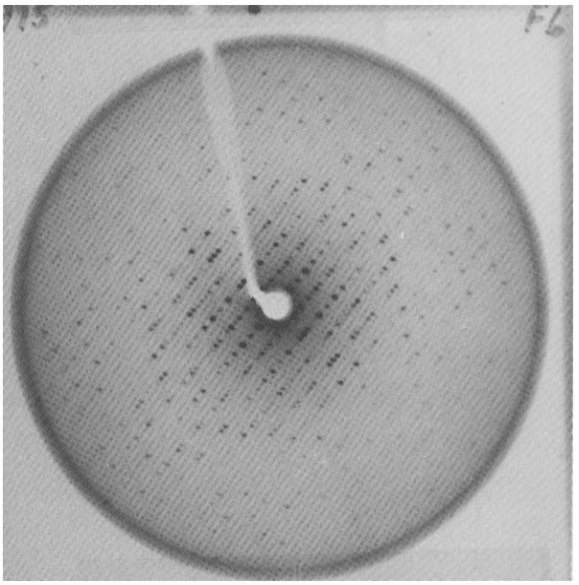

Fig.3. Precession photograph of fragment 1 crystal. Projection *Okl*, precession angle 18 deg. Crystal to film distance 100 mm.

The film densities were measured with an

Table 1

Crystallographic data of fragment 1 from bovine prothrombin

Crystallization conditions:	Polyethylene glycol 6000 8% (w/v)
	Sodium cacodylate 100 mM
	Calcium chloride 100 mM
Protein concentration	25 mg/ml
Cell constants	a = 39.5 Å, b = 54.0 Å, c = 129.0 Å
Space group	$P_12_12_1$
M_r	25 000
Water content	55%
Molecules per asymmetric unit	4
Resolution of data	2.8 Å

Table 2

Summary of statistics connected to data collection out 2.8 Å using rotation geometry and subsequent scaling of redundant data

Compound	No. of films collected	Total no. of reflections	No. of rejected	Unique reflections	$\overline{R_{sym}}$ (%)	$\overline{R_{scale}}$ (%)
Native	33	22 268	885	7431	5.44	7.87
K_2PtCl_6	26	14 164	948	6174	5.89	9.55
$K_2(en)_2Cl_2$	33	20 478	964	6915	5.87	8.29

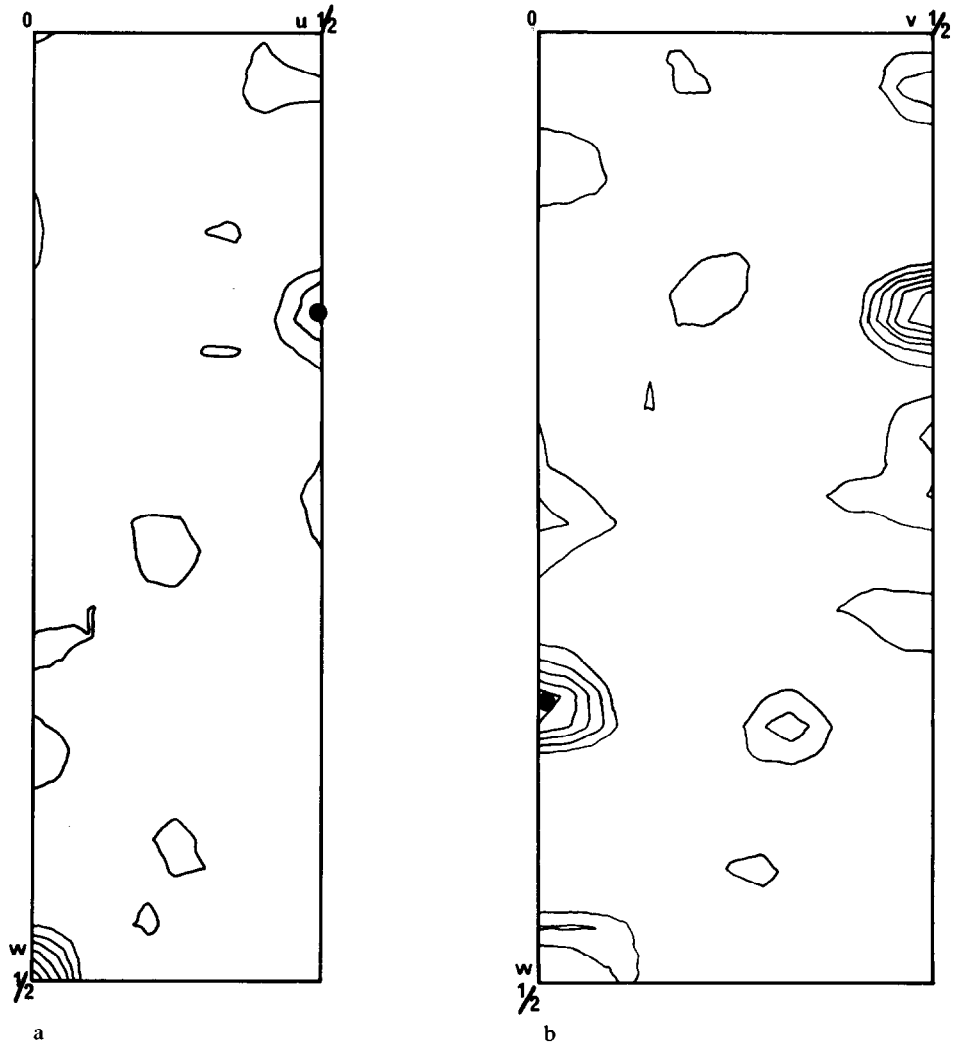

Fig.4. Derivative K_2PtCl_6 Patterson Harker section (a) *uw* at $v = ½$ (*u* across *w* down) and (b) *vw* at $u = ½$ (*v* across *w* down). Major heavy atom site indicated.

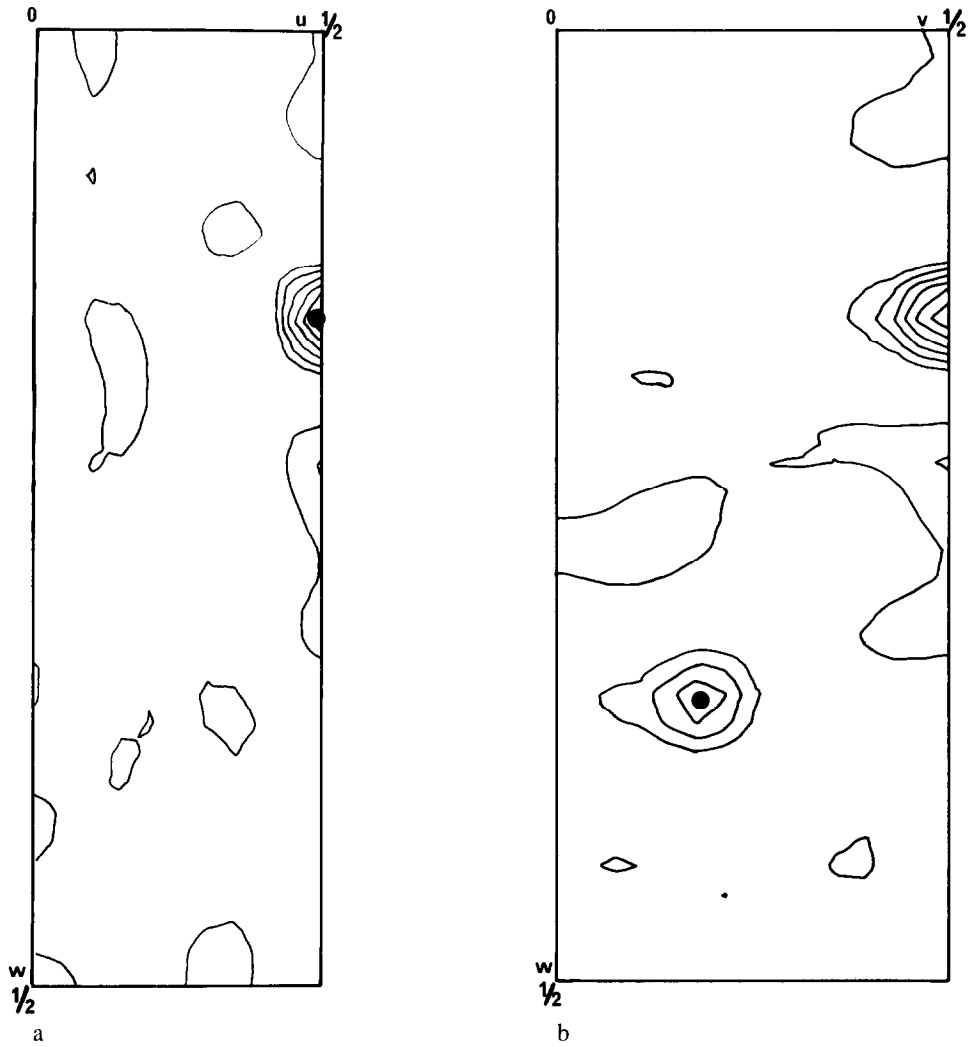

Fig.5. Derivative $K_2Pt(en)_2Cl_2$ Patterson Harker section (a) *uw* at $v = ½$ (*u* across *w* down) and (b) *vw* at $u = ½$ (*v* across *w* down). Major heavy atom site indicated.

Optronics micro densitometer in off-line mode for a subsequent evaluation of integrated intensities on a VAX 11/780 computer. The films obtained in each exposure were scaled together after a non-linearity correction had been applied for each density measured. The different film sets were scaled together using symmetry-related reflections. Scale and temperature factors of each film pack within a complete data set were calculated from fully recorded reflections only. The partially recorded reflections were discarded. The final agreement factors between the symmetry-related amplitudes from the different data sets are given in table 2.

2.3. *Phase determination*

Heavy atom derivatives were prepared by soaking crystals in the standard buffer, containing 8% PEG and the appropriate concentration of heavy atom compound (~10 mM). The heavy atom compounds used in the present calculations were K_2PtCl_6 and $K_2Pt(en)_2Cl_2$ (en = ethylenediamine). Some sixty other compounds were tested without giving any useful derivation [9].

Native and derivative data were brought on an absolute scale using a Wilson plot [10] and difference F^2 functions based on $(|F|_{der}-|F|_{nat})^2$ coefficients were calculated for the derivatives.

Table 3

Phase refinement results for 2132 unique reflections within the resolution of 20.0 to 4.0 Å

Derivative	Site No.	Occupancy	Temperature factor (not refined)	x	y	z
K_2PtCl_6	1	76.86	15.0	.7732	.2363	.3183
	2	56.10	15.0	.5762	.3276	.4614
	3	30.31	15.0	.7205	.2869	.3320
$K_2Pt(en)_2Cl_2$	1	89.33	15.0	.7541	.1614	.3253
	2	74.29	15.0	.7841	.2341	.3192

en = ethylenediamine

Summary of statistics:

Derivative	*Rc*	*RK*	*RL*	*E*	$<F_H>$	$<F_{obs}>$	$<F_{PH}>$	*N*	*Nc*
K_2PtCl_6	68.4	20.8	24.0	100.8	143.4	150.0	376.5	2049	397
$K_2Pt(en)_2Cl_2$	59.3	11.7	14.8	65.6	109.2	118.1	415.5	2083	431

Mean figure of merit: 0.54

E: lack of closure $(\sum_{i=1}^{N} (F_{PH_i}(obs) - F_{PH_i}(calc)^2/N)^{1/2}$

RK: Kraut *R*-factor $100 \cdot [(\sum_{i=1}^{N} | F_{PH_i}(obs) - F_{PH_i}(calc) |)/\sum_{i=1}^{N} F_{PH_i}(obs)]$

Rc: Centric R-factor $RK \cdot (\sum_{i=1}^{N} | F_{PH_i}(obs) | / \sum_{i=1}^{N} | F_{PH_i}(obs) - F_P(obs) |)$ centric reflections only

RL: Least squares *R*-factor $100 \cdot [\sum_{i=1}^{N} | F_{PH_i}(obs) - F_{PH_i}(calc) |^2 / \sum_{i=1}^{N} F^2_{PH_i}(obs)]^{1/2}$

F_P: Structure factor for native protein
F_H: Heavy atom structure factor
F_{obs}: Observed heavy atom structure factor
F_{PH}: Structure factor for protein with heavy atom
N: Number of unique reflections to 4 Å
Nc: Number of centric reflections

The major heavy atom sites were located from Harker sections (figs.4,5). Subsequently the minor sites were found from difference Fourier maps using phases from the major sites.

In order to refer the derivatives to a common origin, cross Patterson synthesis and Fourier maps with phases assigned on the basis of the other derivative were calculated [11]. The heavy atom parameters were refined according to Dickerson [12] and Blow [13]. Table 3 shows the refined heavy atom parameters and some statistics for the refined phases used for the native electron density map to a 4 A.U. resolution.

3. RESULTS

The molecular envelope is readily determined from the 4 A.U. electron density maps. The extensions of the molecule along the crystallographic axes are 39 × 54 × 32 A.U., respectively. The

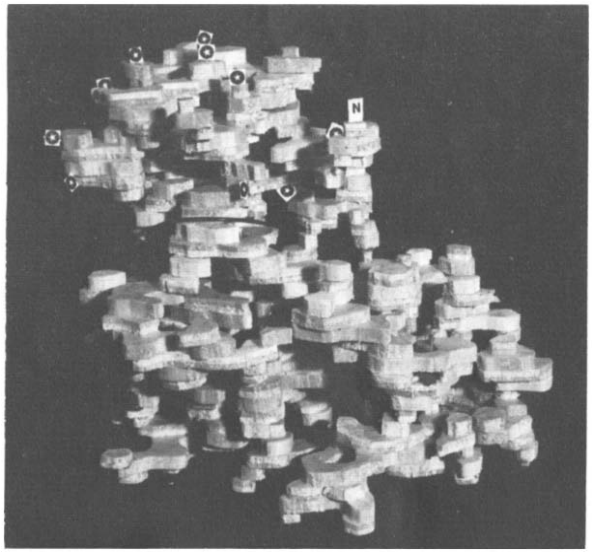

Fig.6. Low resolution model of fragment 1. The approximate positions of the ten γ-carboxy glutamic acids and the N-terminus are indicated.

density maps show that the molecule contains very few regions with secondary structures if any at all.

The molecule as shown in fig.6 consists roughly of two domains separated by a cleft. The smaller part, about one third of the molecule and located at the N-terminus end, also contains the γ-carboxy glutamic acids. These modified residues are situated on the surface of the molecule, probably exposing their carboxy groups. Whether or not they bind any Ca^{2+} cannot be decided uniquely from the present maps, although high densities occur in the vicinity. The smaller domain also contains one of the five disulfide bridges, which together with the residues 19–22 form a globular bulb on the surface of the molecule.

The larger domain has density regions indicating that this part of the molecule is rather compact. It contains the remaining four S–S bridges, and two of them, Cys 87–Cys 127 and Cys 115–Cys 139 are located in the middle of this domain. There are still some doubts regarding the locations of the other two S–S bridges.

At a 4 A.U. resolution level, it is difficult to distinguish between carbohydrate and amino acid residues. Inspecting the maps, it seems as if the two carbohydrate sites are located one on each side of the molecule. These regions show either poor density or discontinuous density peaks, indicating that some regions in the carbohydrate sites may not be well ordered.

Work with phase extension to 2.8 A.U. is in progress.

ACKNOWLEDGEMENTS

G.O. wishes to thank Professor R. Huber at the Max-Planck Institute of Biochemistry, Munich, Federal Republic of Germany for the possibility to use his equipment to collect the film data and to evaluate the intensities. The project has been supported by the Swedish Natural Science Research Council (NFR).

REFERENCES

[1] Magnusson, S., Sottrup-Jensen, L., Petersen, T.E. and Clayes, H. (1975) in: Prothrombin and Related Coagulation Factors (Hemker, H.C. and Veltkamp, J.J., eds) pp. 25–46, Leiden University Press, Leiden.
[2] Esnouf, M.P. and MacFarlane, R.G. (1968) in: Advances in Enzymology (Nord, F.F., ed.) Vol. 30, pp. 255–315, Interscience, New York.
[3] Nelsestuen, G.L. (1976) J. Biol. Chem. 251, 5648–5656.
[4] Henriksen, R.A. and Jackson, C.M. (1975) Arch. Biochem. Biophys. 170,149–159.
[5] Lagerkvist, U., Rymo, L., Lindqvist, O and Andersson, E. (1972) J. Biol. Chem. 247, 3897–3899.
[6] Aschaffenburg, R., Blake, C.C.F., Burridge, J.M. and Esnouf, M.P. (1977) J. Mol. Biol. 114, 575–579.
[7] Hu Kung, W.J. and Tulinsky, A. (1979) in: The Regulation of Coagulation (Mann, K.G. and Taylor, F.B., eds.) pp. 81–88, Elsevier Biomedical, Amsterdam, New York.
[8] Arndt, U.W. and Wonacott, A.J. (1977) in: The Rotation Method in Crystallography (Arndt, U.W. and Wonacott, A.J., eds.) pp. 5–18, Elsevier Biomedical, Amsterdam, New York.
[9] Olsson, G. (1981) Thesis, University of Göteborg.
[10] Wilson, A.J.C. (1949) Acta Cryst. 2, 318–321.
[11] Rossmann, M.G. (1960) Acta Cryst. 13, 221–226.
[12] Dickerson, R.E., Weinzierl, J.E. and Palmer, R.A. (1968) Acta Cryst. B24, 997–1003.
[13] Blow, D.M. and Crick, F.H.C. (1959) Acta Cryst. 12, 794–802.